

Multireference singles and doubles configuration interaction study of the photoelectron spectrum of HO- 2

Gabriel J. Vazquez, Robert J. Buenker, and Sigrid D. Peyerimhoff

Citation: *The Journal of Chemical Physics* **90**, 7229 (1989); doi: 10.1063/1.456252

View online: <http://dx.doi.org/10.1063/1.456252>

View Table of Contents: <http://scitation.aip.org/content/aip/journal/jcp/90/12?ver=pdfcov>

Published by the AIP Publishing

Articles you may be interested in

[Cholesky decomposition within local multireference singles and doubles configuration interaction](#)

J. Chem. Phys. **132**, 074104 (2010); 10.1063/1.3315419

[Linear scaling multireference singles and doubles configuration interaction](#)

J. Chem. Phys. **128**, 224106 (2008); 10.1063/1.2937443

[Local correlation in the virtual space in multireference singles and doubles configuration interaction](#)

J. Chem. Phys. **118**, 8127 (2003); 10.1063/1.1565314

[Pseudospectral multireference single and double excitation configuration interaction](#)

J. Chem. Phys. **102**, 7564 (1995); 10.1063/1.469088

[Size consistent multireference single and double excitation configuration interaction calculations. The multireference coupled electronpair approximation](#)

J. Chem. Phys. **94**, 7212 (1991); 10.1063/1.460204



Multireference singles and doubles configuration interaction study of the photoelectron spectrum of HO_2^-

Gabriel J. Vazquez^{a)}

Instituto de Física, Universidad Nacional Autónoma de México, Cuernavaca Group, AP-139B, 62190 Morelos, México

Robert J. Buenker

Lehrstuhl für Theoretische Chemie, Bergische Universität-GH Wuppertal, Gaußstraße 20, D-5600 Wuppertal 1, West Germany

Sigrid D. Peyerimhoff

Lehrstuhl für Theoretische Chemie, Universität Bonn, Wegelerstraße 12, D-5300 Bonn 1, West Germany

(Received 24 March 1988; accepted 4 January 1989)

Multireference singles and doubles configuration interaction (MRD-CI) electronic structure calculations are carried out on the hydroperoxyl radical and its negative ion. Potential energy curves of the ground state of the anion and of the ground and first excited states of the neutral molecule along the O–OH coordinate are employed to compute the Franck–Condon factors for the electron photodetachment processes $\text{HO}_2(X^2A'', A^2A') + e \leftarrow \text{HO}_2^-(X^1A')$. The theoretical spectrum agrees fairly well with the photoelectron spectrum reported by Oakes, Harding, and Ellison, and is consistent with their assignment of the peaks K and D as origins for the electron loss transitions to the $\text{HO}_2 A$ and X states, respectively. An alternative choice of peak E as $X \leftarrow X^-$ origin yields better agreement between computed and experimental Franck–Condon factors than does the peak D assignment, but is less satisfactory when energetic considerations are taken into account. Two independent *ab initio* results lend support to the value of 1.078 ± 0.017 eV for the measured adiabatic electron affinity of HO_2 , which is in good agreement with the best value inferred from the MRD-CI calculations of 1.069 ± 0.05 eV. The matter is not settled, however, as some inconsistencies in the experimental data still cast some doubts on the assignment of the peaks and the accuracy of the HO_2 EA.

I. INTRODUCTION

The hydroperoxyl radical HO_2 plays an important role as an intermediate in a variety of chemical reactions, such as in combustion, atmospheric, and biological processes,^{1–3} both in the gas phase and in solution. Given its relevance and ubiquitous nature there continues to be a great deal of interest in this species. Hence, over the past few years, we have been engaged with various aspects of this radical and related species, including the HO_2 UV photochemistry, in particular photodissociation,⁴ the electronic structure of the HO_2^+ cation,⁵ and, very recently, with the HO_2 electron affinity (EA) and corresponding HO_2^- electron photodetachment energy (PDE).⁶ The various dissociation products of the neutral, cationic, and anionic systems have also been dealt with explicitly in these papers.

Unlike the neutral and positive species, for which there is a considerable amount of spectroscopic and kinetic data available, relatively little is known about the hydroperoxyl radical anion. Until recently most of the information available was to a good extent collateral, mainly in the form of estimates of the electron affinity of the neutral molecule. Clearly, the precise knowledge of this quantity is of major significance for the assessment of the energetics of numerous reactions involving compounds containing oxygen and hydrogen. A wide range of values has been reported for this quantity, however, and the question of the actual value of the HO_2 EA is not yet settled. There is a disagreement between the two most reliable experimental values, for example,

namely 1.19 ± 0.01 eV obtained in a photodetachment experiment⁷ and 1.078 ± 0.017 eV resulting from the assignment of the photoelectron spectrum.⁸ On the other hand, recent calculations⁶ indicate that the EA(HO_2) is 1.069 ± 0.05 eV, a value which is in better agreement with the results of Oakes *et al.*⁸ An overview of previous HO_2 EA estimates and a more detailed discussion of the vertical and adiabatic HO_2 electron affinities and HO_2^- photodetachment energies can be found in Ref. 6.

Other features of the hydroperoxyl radical anion have been revealed over the past decade. It has become clear that HO_2^- is a potent oxidizing agent which can be employed as a base. In the gas phase, for example, it is known to readily oxidize CO, NO, CO_2 , etc.⁹ It also appears to be important in the aqueous chemistry of ozone.³ There is also evidence that it might be involved in a number of other reactions. For example, it has also been suggested that the initial step in low temperature ($T < 450^\circ\text{C}$) hydrocarbon combustion may proceed via an ion-pair intermediate involving the HO_2^- anion.³ Theoretical calculations also indicate the possibility of HO_2^- involvement in the enzymatic oxidation/reduction of the superoxide anion O_2^- .¹⁰ Very recently the UV molar absorptivities of aqueous HO_2^- and H_2O_2 have been measured in the range 200–300 nm.¹¹ As for theoretical calculations, three previous studies have yielded equilibrium geometries in good agreement with each other^{6,8,12} and also with the measured O–O bond length, the only geometrical parameter which has been determined experimentally so far.⁸ The HO_2 electron affinity has proved particularly difficult to calculate, however, as has been found to be the case for a number

^{a)} Alexander von Humboldt fellow, West Germany.

of other oxygen-containing species.⁶ The fundamental vibrational frequencies of HO₂⁻ have also been reported.^{6,8} The computed $\nu_3(\text{O-OH})$ vibrational fundamental of 833⁶ and 821 cm⁻¹⁸ agree with the experimental counterpart of 775 ± 250 cm⁻¹,⁸ but the large error bars in the measured value make the comparison uncertain.

The HO₂⁻ photoelectron spectrum recently reported by Oakes, Harding, and Ellison⁸ shows relatively well-resolved vibrational structure which has been assigned by these authors. In the present contribution we report a theoretical PE spectrum which is compared with the available measurements. A discussion of the assignment of the vibrational features is undertaken based on the experimental and theoretical evidence. MRD-CI electronic structure calculations are carried out on the three electronic species which are involved in the HO₂⁻ photodetachment process, namely, the ground state of the anion ($X^{-1}A'$) and the ground ($X^{-2}A''$) and first excited ($1^{-2}A'$) states of the neutral molecule. The major portion of the analysis of the spectrum is based on the Franck-Condon factors (FCFs) which are obtained from cuts of the potential energy surfaces along the active mode, O-OH.

II. DETAILS OF THE CALCULATIONS

Ab initio SCF MRD-CI electronic structure calculations have been carried out on the HO₂⁻ ($X^{-1}A'$), HO₂ ($X^{-2}A''$), and HO₂ ($A^{-2}A'$) states which subsequently will be referred to as X^{-} , X , and A , respectively. In this paper we report a cut of the potential energy surfaces of X^{-} , X , and A along the O-OH coordinate. It will be shown later on that the HO₂⁻ PE spectrum can be understood largely on the basis of this mode alone. Two AO basis sets are employed. Basis A is of double-zeta plus polarization quality augmented with s and p bond and Rydberg functions; this is the same basis used in a previous study on HO₂ and HO₂⁺ and further details can be found in Refs. 4 and 5. Basis B differs from A through the addition of a set of p negative ion functions ($\alpha_p = 0.059$) on each of the oxygen atoms. The negative ion curve was calculated with the largest AO basis B , whereas the curves of the neutral states X and A are calculated with basis A . Basis B and A consist, respectively, of 52 and 46 contracted Gaussian functions. The two deepest-lying molecular orbitals (MOs) corresponding to the $1s$ shells of the oxygen atoms were kept doubly occupied in all calculations and their complements in the virtual space were disregarded. The active spaces of bases B and A are hence 48 and 42 MOs, in which the remaining 14 electrons are allowed to be distributed. The calculations are carried out in C_s symmetry. The configuration interaction treatment was carried out with the MRD-CI set of programs.¹³⁻¹⁶ The potential curves of the X and A states were calculated with a threshold of $10 \mu\text{hartree}$, whereas $T = 15 \mu\text{hartree}$ was taken for the calculations of the X^{-} curve.

The differences in the treatments of neutral and ionic systems result in part from the fact that the neutral curves X and A were actually taken from a previous study.⁴ The important point to stress in this respect is that in spite of the slight differences the computed X^{-} , X , and A potential energy curves appear to be suitable for the discussion of the HO₂⁻

TABLE I. Calculated equilibrium O-OH bond lengths and corresponding vibrational frequencies for the X^{-} , X , and A states.

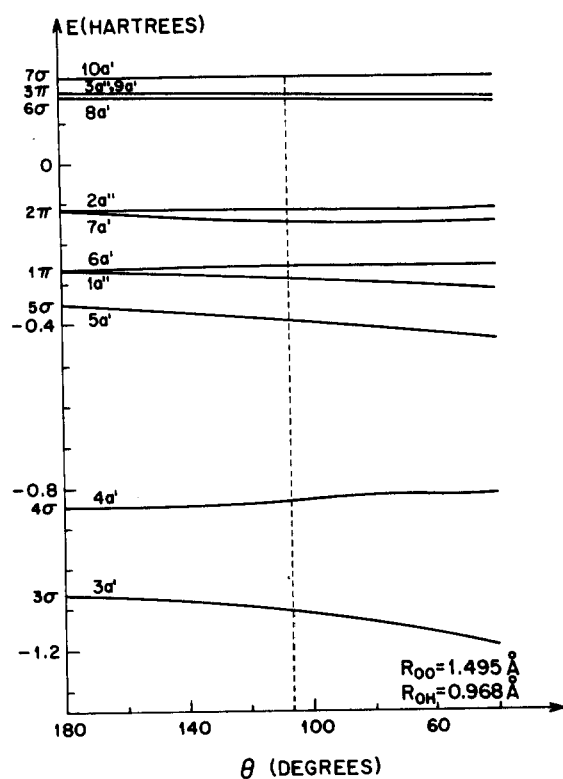
State	$R_e(\text{O-OH}) \text{ \AA}$	$\nu_3(\text{O-OH}) \text{ cm}^{-1}$
HO ₂ ($A^{-2}A'$)	1.405	978.6
HO ₂ ($X^{-2}A''$)	1.345	1131
HO ₂ ⁻ ($X^{-1}A'$)	1.495, 1.499 ^a	833

^aThe value $R_e(\text{O-OH}) = 1.499 \text{ \AA}$ resulted from a more careful calculation with supplementary points in the potential.

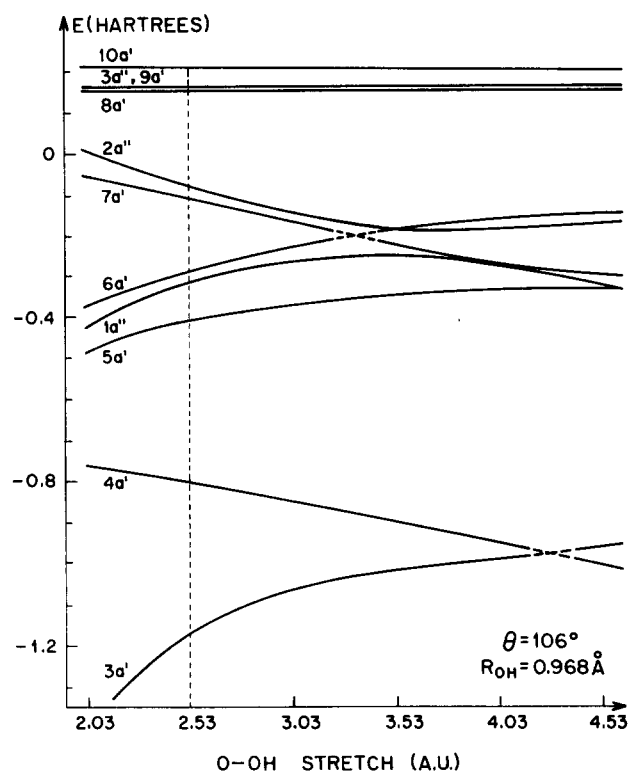
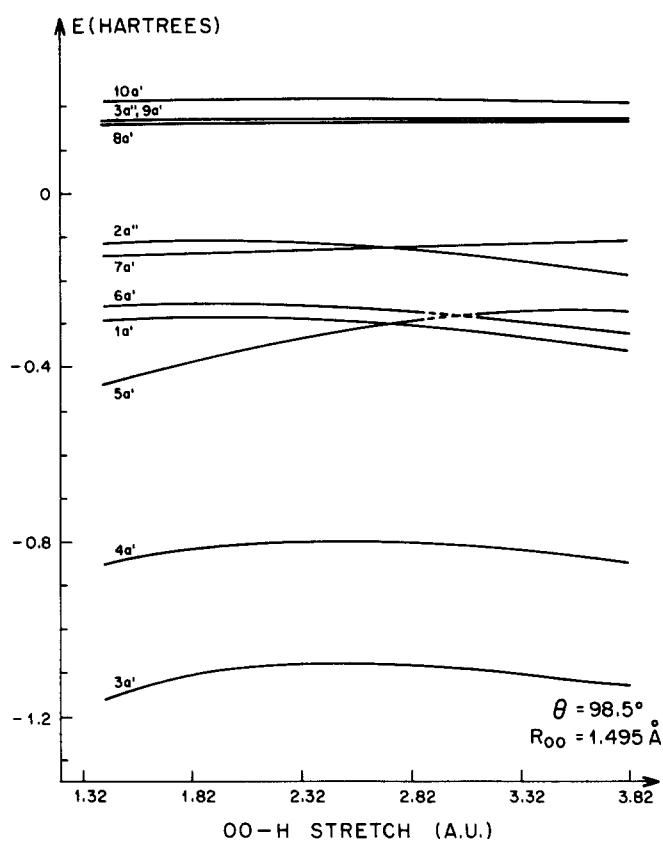
PES. In particular, the calculated O-OH equilibrium bond lengths as well as the shapes of the curves (which are the dominant factors for the computation of the FCFs) seem to have been properly accounted for in the calculations. This position appears justified considering the good agreement encountered between calculated and experimental equilibrium geometries and fundamental vibrational frequencies. It is also worth noting that our estimate of the adiabatic HO₂ electron affinity of 1.069 ± 0.05 eV reported in a companion paper,⁶ which is relevant to the ensuing discussion of the HO₂⁻ PES, results from a series of calculations on three other anion-neutral pairs, namely, O⁻-O, OH⁻-OH, O₂⁻-O₂, as well as HO₂⁻-HO₂. The calculations of these eight systems were carried out in a consistent manner (at their respective experimental equilibrium geometries) by employing AO basis sets C and D , which are larger than basis B and differ from it through the addition of a set of d (basis C) and a set of d plus a set of f (basis D) negative ion functions on each of the oxygen atoms. All these computations were carried out with a CI threshold of $10 \mu\text{hartree}$. The calculated O-OH equilibrium bond lengths and corresponding vibrational fundamentals of X^{-} , X , and A are given in Table I. The vibrational Schrödinger equation has been solved for the O-OH mode without consideration of perturbations exerted by the © and O-H modes, i.e., by employing an independent-mode model.

III. MOLECULAR ORBITALS AND ELECTRONIC CONFIGURATIONS

Molecular orbital energy level diagrams of HO₂⁻ along the bending, O-OH and OO-H coordinates are given in Figs. 1-3. The data are taken from ground state SCF calculations on HO₂⁻ carried out employing basis B . The anion contains 18 electrons with the first seven MOs of a' symmetry as well as $1a''$ and $2a''$ being doubly occupied in the ground electronic state. The bent-linear correlation of these orbitals is given in Fig. 1. For example, the ($7a', 2a''$) pair are the components of the antibonding 2π MO of the linear molecule and the pair ($1a'', 6a'$), the components of the bonding 1π MO. Occupation of $3a', 5a', 1a''$, and $7a'$ slightly favors small bond angles, whereas occupation of $4a', 6a'$, and $2a''$ slightly favor the linear geometry. All the occupied MOs are quite sensitive to O-OH stretching (Fig. 2). Population of ($7a', 2a''$) 2π and ($4a'$) 4σ , favors long O-O internuclear distances while the opposite (bonding) behavior is shown by the ($1a'', 6a'$) 1π , ($5a'$) 5σ , and ($3a'$) 3σ MOs, especially the latter whose energy drops steeply as the O-OH distance decreases. An interesting feature of Fig. 2 is the avoided cross-

FIG. 1. Energetical behavior of the HO_2^- MOs with bending.

ing involving the antibonding $7a'$ MO with the bonding $6a'$ near 3.4 bohr. Along the OO-H coordinate all occupied MOs are relatively insensitive to stretching, with the exception of $5a'$ which is clearly O-H bonding (Fig. 3). This orbi-

FIG. 2. Energetical behavior of the HO_2^- MOs with stretching of the O-OH bond.FIG. 3. Energetical behavior of the HO_2^- MOs with stretching of the OO-H bond.

tal is involved in avoided crossing with $6a'$ near 3.0 bohr. Generally speaking the virtual orbitals $8a'$, $9a'$, $10a'$, and $3a''$ which are unoccupied in the ground state are insensitive to geometry changes (Figs. 1-3), thus indicating their diffuse character.

The ground state of HO_2^- is hence $X^1A'(\dots 5a'^2 1a''^2 6a'^2 7a'^2 2a''^2)$. The ground electronic state of the neutral molecule is $X^2A''(\dots 7a'^2 2a''^2)$ and results from the loss of a single electron out of the HOMO of the anion, i.e., from the $2a'' \rightarrow \infty$ ionization. Electron detachment out of the second highest occupied MO ($7a'$) results in the neutral molecule in its first excited state $A^2A'(\dots 6a'^2 7a' 2a''^2)$. The electronic configurations of X^- , X , and A are illustrated in Fig. 4.

IV. THE HO_2^- PHOTOELECTRON SPECTRUM

Before undertaking the description of the HO_2^- PES it is worthwhile to review some details regarding the measurements of Oakes, Harding, and Ellison.⁸ The HO_2^- anion was produced in the reaction $\text{HNO}^- + \text{O}_2 \rightarrow \text{HO}_2^- + \text{NO}$, whereby HNO^- is obtained from ethyl nitrite. The HO_2^- anion is then accelerated and mass selected in a high pressure spectrometer. The emerging ion beam is crossed by a cw Ar II laser of fixed frequency $\lambda_0 = 488 \text{ nm}$ (2.540 eV), bringing about the detachment of one of the electrons of HO_2^- . These electrons are then counted and energy analyzed, and the plot of total electron counts vs the center-of-mass (c.m.) kinetic energy (KE) comprises the PE spectrum.

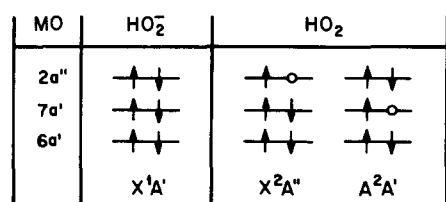


FIG. 4. Electronic configurations of the states involved in the HO₂⁻ photo-detachment process yielding the PE spectrum.

The photoelectron spectrum of HO₂⁻ obtained by Oakes *et al.* (see Fig. 5 of Ref. 8) displays a well-resolved vibrational structure consisting of 13 peaks (labeled C through O) in the KE range 0–1.5 eV. The c.m. KE of each peak, as well as the energy interval between successive peaks is given in Table II. The overall intensity pattern of the peaks suggests that the HO₂⁻ PE spectrum is composed of two different band systems. One of them would seem to encompass the vibrational envelope consisting of peaks C–J; the intensity rises smoothly and progressively from peak C to a maximum at peak G, and then decreases smoothly again until peak J is reached. The sudden and sharp increase in intensity for peak K would then seem to indicate the onset of another band, the break between the two bands apparently lying somewhere between peaks J and K. The members of the second vibrational progression would then be peaks K–O, with their intensities steadily decreasing from the maximum at peak K. Evidently the electron photodetachment in HO₂⁻ is occur-

TABLE II. Center-of-mass kinetic energy and energy splittings for the leading vibrational features in the HO₂⁻ PE spectrum (Ref. 8).

Peak	KE (eV) ^a	ΔE	
		eV	cm ⁻¹
C	1.503 ± 0.019	0.093	750
D	1.407 ± 0.024	0.112	903
E	1.295 ± 0.018	0.123	992
F	1.172 ± 0.009	0.133	1072
G	1.039 ± 0.013	0.127	1024
H	0.912 ± 0.009	0.130	1048
I	0.782 ± 0.017	0.109	879
J	0.673 ± 0.019	0.083	669
K	0.590 ± 0.013	0.123	992
L	0.467 ± 0.013	0.119	960
M	0.348 ± 0.018	0.120	968
N	0.228 ± 0.019	0.080	645
O	0.148 ± 0.024		

^a The energy of the vibrational features in the photoelectron spectrum corresponds to the center of gravity of the peaks, as it was not possible to resolve their underlying rotational or spin-orbit structure (Ref. 20).

ring to at least two distinct electronic species of the neutral molecule.

V. COMPARISON OF THE CALCULATED RESULTS WITH EXPERIMENTAL DATA

A. Computed potential energy curves and identification of the species involved in the photoelectron spectrum

The calculated potential energy curves of X⁻, X, and A along the O–OH coordinate which will be employed for the computation of the HO₂⁻ PES are shown in Fig. 5. The calculated adiabatic HO₂(X) EA of 0.68 eV estimated from them is roughly 0.4 eV too small relative to the photoelectron value of 1.078 eV,⁸ very likely because the computed X⁻ curve is not deep enough relative to the neutral curves X and A. It is well known that such large differences between computed and measured EAs are not uncommon, however; e.g., a survey of the most elaborated theoretical EA calculations available on the oxygen atom and other simple oxygen-containing compounds has shown that theory underestimates electron affinities by a considerable amount (0.1–0.5 eV) depending upon the treatment.⁶ The present underestimation of 0.4 eV is thus in line with what one would have expected given the AO basis and correlation treatment employed [notice, however, that an adiabatic HO₂(X) EA of 0.757 eV was obtained from calculations at the equilibrium geometries of X and X⁻ employing the largest basis set D, thus yielding an error of only 0.3 eV⁶]. We have assumed that the 0.4 eV differential error between anionic and neutral systems is constant for the range of geometries considered in

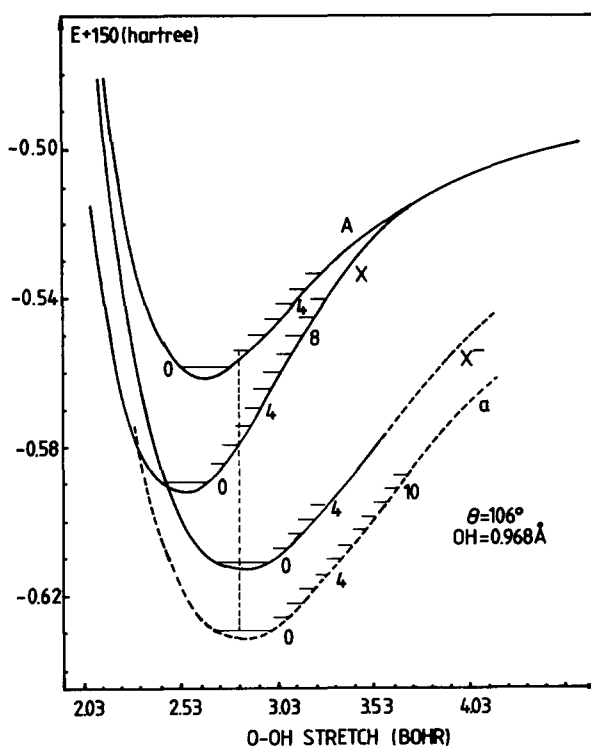


FIG. 5. Calculated O–OH stretching potential energy curves of the three electronic species involved in the HO₂⁻ photoelectron spectrum. The dashed negative ion curve *a* together with the X and A curves give a more realistic representation of the relative positions of these state (see the text).

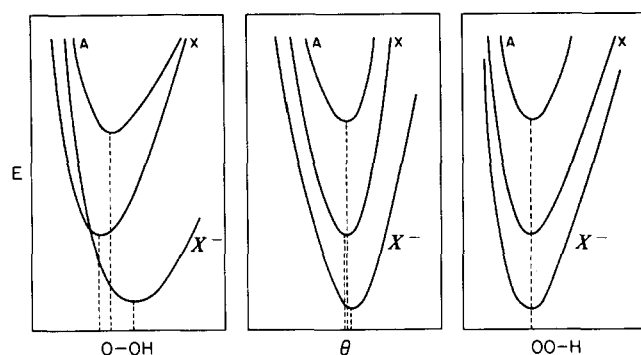


FIG. 6. Illustration of the geometrical changes associated with the HO₂⁻ photodetachment process (schematic).

Fig. 5 and we have accordingly shifted the X⁻ curve downwards to correspond to an EA value of 1.078 eV. The dashed negative ion curve (a) together with the neutral X and A curves therefore constitute a more realistic representation of the relative energetics of the electronic states involved in the HO₂⁻ PD process.

The identity of the HO₂ electronic states involved is evident from Fig. 5, as there are only two of them which are of sufficiently low energy, the ground state X²A'' and the first excited state 1²A'. The next excited state, 1⁴A'' at about 6 eV,⁴ lies much too high and thus the involvement of more than two neutral species in the spectrum is excluded. Consequently there is no question that the vibrational progression on the high (right) KE side of the spectrum with intensity maximum at peak G corresponds to the X²A'' state, while that at the low KE side with maximum at peak K is due to 1²A'.

B. Identification of the active mode in the HO₂⁻ PES

Electronic transitions in polyatomic molecules usually selectively excite only one (or at most a few) of the 3N - 6 (or 3N - 5) vibrational modes, and this is referred to as the active mode. Generally, the mode which is excited is the one which undergoes a considerable geometry change in the excitation process. The behavior of the HO₂⁻ (X⁻) and HO₂(X,A) states along the O-OH, Θ, and OO-H coordinates is shown schematically in Fig. 6 allowing for an easy

identification of the active mode in the PE spectrum of HO₂⁻. A key feature in this figure is the fact that the X and A curves are substantially shifted with respect to the X⁻ curve along the O-OH coordinate, whereas along Θ and OO-H the neutral and ionic curves are nearly parallel. The corresponding experimental equilibrium geometries (selected values are summarized in Table III) illustrate these trends numerically. The value of R(O-O) changes considerably in going from anion to neutral, from 1.499 to 1.330 and 1.393 Å, respectively, for X and A. Conversely, the changes in the other two modes are small: Θ is 98.5° (X⁻) compared to 104.29° (X) and 102.69° (A) and R(O-H) is 0.956 Å (X⁻), nearly the same as 0.9707 Å (X) and 0.9654 Å (A). The shortening of the O-O bond in the PD process is also in line with what one would expect from qualitative MO theory,^{17,18} since the photoejected electron, either 2a'' or 7a', is O-O antibonding in both cases.

According to the discussion above one would thus expect O-OH to be the active mode in the HO₂⁻ PES, and this conclusion is confirmed by the size of the spacings between successive peaks (Table II). The mean energy interval between peaks F-E, G-F, H-G, and I-H (which almost certainly involve the X state), is 0.128 eV or 1034 cm⁻¹ and that between peaks L-K, M-L, and N-M (which should correspond to the A state) is 0.120 eV or 973 cm⁻¹. These figures are fairly close (although certainly not identical) to the ν₃(O-O) fundamentals of X²A'' (1101 cm⁻¹) and 1²A' (926 or 985 cm⁻¹; Table III). The ν₂(Θ) and ν₁(O-H) characteristic vibrational frequencies are much higher: 1390 and 3436 cm⁻¹ for X, 1285 and 3268 cm⁻¹ for A. This information led Oakes *et al.* to conclude that ν₃(O-O) is the active mode in the PES. Furthermore, no structure was found which could be attributed to the Θ or O-H vibrational modes,⁸ in agreement with what one would expect given the shape of the computed potential energy curves illustrated in Fig. 6.

C. Computed Franck-Condon factors for the photodetachment process

The prediction of the spectrum (vibrational features) associated with an electronic transition involves the calculation of the intensity (in absorption):

TABLE III. Equilibrium geometry and fundamental vibrational frequencies of the species involved in the HO₂(X,A) ← HO₂⁻ (X⁻) photodetachment process.

System	O-O stretch		Bending		O-H stretch	
	R _e (Å)	ν ₃ (cm ⁻¹)	θ (deg)	ν ₂ (cm ⁻¹)	R _e (Å)	ν ₁ (cm ⁻¹)
HO ₂ (A ² A')	1.393 ^{3a}	984.8, ^a 926 ^d	102.69 ^a	1285 ^a	0.9654 ^a	3268.5 ^a
HO ₂ (X ² A'')	1.330 ^{54b}	1101 ^c	104.29 ^b	1390 ^a	0.9707 ^b	3436.1951 ^f
HO ₂ ⁻ (X ¹ A')	1.499 ^c	883 ^c	98.5 ^c	1170 ^c	0.956 ^c	3650 ^c

^a Reference 19.

^b K. G. Lubic, T. Amano, H. Vehara, K. Kawaguchi, and E. Hirota, *J. Chem. Phys.* **81**, 4826 (1984).

^c This work.

^d K. J. Holstein, E. H. Fink, and F. Zabel, *J. Mol. Spectrosc.* **99**, 231 (1983).

^e M. E. Jacox and D. E. Millikan, *J. Mol. Spectrosc.* **42**, 495 (1972).

^f C. Yamada, Y. Endo, and E. Hirota, *J. Chem. Phys.* **78**, 4379 (1983).

$$I_{v',v''} = DN_{v''} E_{v',v''}^4 \left[\int \psi_{v'} R_{e'e''}(r) \psi_{v''} dr \right]^2$$

of each of the $v' \leftarrow v''$ vibronic transitions which encompasses the band, where D is a constant, $N_{v''}$ stands for the population of the v'' levels, $E_{v',v''}$ is the energy of the transition, $\psi_{v'}$ and $\psi_{v''}$ are vibrational wave functions, and $R_{e'e''}$ is the electronic transition moment. The computation of the vibrational transition probability $[\int \psi_{v'} R_{e'e''}(r) \psi_{v''} dr]^2$ has been simplified, so that the evaluation of the electronic transition moment for an ionization process is omitted. It is simply assumed that this quantity is essentially constant over the geometrical range of interest. In the context of this approximation

$$I_{v',v''} \propto \left[\int \psi_{v'} \psi_{v''} dr \right]^2,$$

that is, the intensity of a given $v' \leftarrow v''$ transition is merely proportional to the corresponding Franck-Condon factor (FCF).

At this point it is worthwhile to recall a number of details regarding the FCFs which will prove useful for the subsequent discussion of the HO₂⁻ PES. (1) The FCFs depend only on the relative shapes and equilibrium positions of the curves involved in the photodetachment process and not of their relative position in the energy scale; (2) the range of internuclear distances in which $R_{e'e''}$ is assumed to be constant is roughly 1.1 bohr in the present case, namely, from the left vibrational turning point HO₂($X, v' = 8$) at about 2.1 bohr, to the right turning point of HO₂⁻($X^-, v'' = 3$) at about 3.2 bohr (see Fig. 5); (3) since the initial vibrational population $N_{v''}$ is unknown, the only meaningful comparison one can make between measured and calculated FCFs is along progressions stemming from the same v'' level. The relative intensities of the various transitions in the $v' \leftarrow v'' = \text{constant}$ progressions can be obtained immediately from the FCFs (even without knowing $N_{v''}$), but there is no way of establishing a relationship between those stemming from a different v'' unless the relative population $N(v''_1)/N(v''_2)$ is known; (4) the FCFs by themselves do not enable the comparison of relative intensities between different band systems since $R_{e'e''}$ is normally different for each electronic transition. Consequently, the computed FCFs for the $X \leftarrow X^-$ and $A \leftarrow X^-$ systems do not provide information about the relative strengths of the two bands. Nonetheless, within each band system, the calculated FCFs can be translated into relative intensities which are quite useful for the purpose at hand.

We have calculated the FCFs for the HO₂(X, A) \leftarrow HO₂⁻(X^-) PD reaction in the context of the independent mode approximation. We employ the curves of X^- , X , and A along the O-OH coordinate (Fig. 5) to compute the FCFs associated with the active mode ν_3 (O-O). Those associated with the nonactive modes, Θ and OO-H, were not treated since they are practically irrelevant for the discussion of the PES. The calculations were carried out separately for each of the bands, $X \leftarrow X^-$ and $A \leftarrow X^-$, and the FCFs for transitions arising from $v'' = 0, 1, 2, 3$ of HO₂⁻(X^-) to various vibrational levels of HO₂(X) and HO₂(A) are given in a Deslandres-like diagram (Table IV). The computed FCFs of the "cold" photodetachment process HO₂($X, A; v' \geq 0$) \leftarrow HO₂⁻($X^-, v'' = 0$) are plotted in Fig. 7 together with the FCFs obtained by Oakes *et al.* from the measured spectrum.⁸ We shall see in Sec. VI that transitions starting from $v'' = 0$ dominate the spectrum. Accordingly, these FCFs are particularly useful for the assignment of the spectral peaks. The FCFs for transitions originating in excited vibrational levels of the lower state are discussed separately in a paragraph devoted to the possible role of hot bands in the spectrum (Sec. VII).

D. Previous and present assignments of the HO₂⁻ PES

In the present paragraph we first review previous assignments for the vibrational structure of the spectrum shown in Fig. 5 of Ref. 8 and subsequently we put forward the assignments suggested by the present FCF calculations. We have already mentioned that the two distinct FC envelopes in the spectrum correspond to HO₂⁻ electron detachment in the X and A states of HO₂, whereby peaks C-J presumably belong to X and peaks K-O to A . The primary question is which of the peaks correspond to the origins of the X and A states as this fixes the assignment of the vibrational structure and hence the interpretation of the spectrum.

A first consideration regarding the origins of X and A may be taken from the work of Bierbaum *et al.*,⁷ who measured the adiabatic onset of photodetachment to the A state to be 2.06 eV. Subtracting this result from the photon energy (2.54 eV) of the laser employed by Oakes *et al.*⁸ yields 0.48 eV for the KE value at which the (0,0) $A \leftarrow X^-$ transition should occur based on the photodetachment results. Accordingly from Table II, either one of peaks K (0.590 eV) or L (0.467 eV) could be taken as the origin of A . Since the X state origin is accurately known to lie 0.871 eV below that of the A state,¹⁹ the onset of photodetachment to the neutral

TABLE IV. Calculated FCFs^a for the lowest vibronic transitions in the photodetachment process HO₂($X, A; 0 < v' < 8$) \leftarrow HO₂⁻($X^-; v'' = 0-3$).

HO ₂ ⁻ (X^-)	HO ₂ (X, A) ^b								
	$v' = 0$	1	2	3	4	5	6	7	8
$v'' = 0$	0.23(0.85)	0.72(0.93)	1.00(0.39)	0.86(0.07)	0.52(0.00)	0.23(0.00)	0.08(0.00)	0.02(⋯)	0.00(⋯)
1	0.56(0.75)	0.72(0.00)	0.15(0.66)	0.06(0.65)	0.51(0.17)	0.71(0.01)	0.54(0.00)	0.27(⋯)	0.10(⋯)
2	0.75(0.40)	0.22(0.35)	0.12(0.13)	0.51(0.33)	0.17(0.76)	0.04(0.26)	0.44(0.10)	0.65(⋯)	0.48(⋯)
3	0.72(0.16)	0.00(0.45)	0.44(0.07)	0.10(0.28)	0.17(0.15)	0.43(0.80)	0.07(0.31)	0.11(⋯)	0.52(⋯)

^a Normalized to the experimental FCF of peak G for the X state and to the FCF of peak K for the A state (see the text).

^b The FCFs corresponding to the A state are given in parentheses.

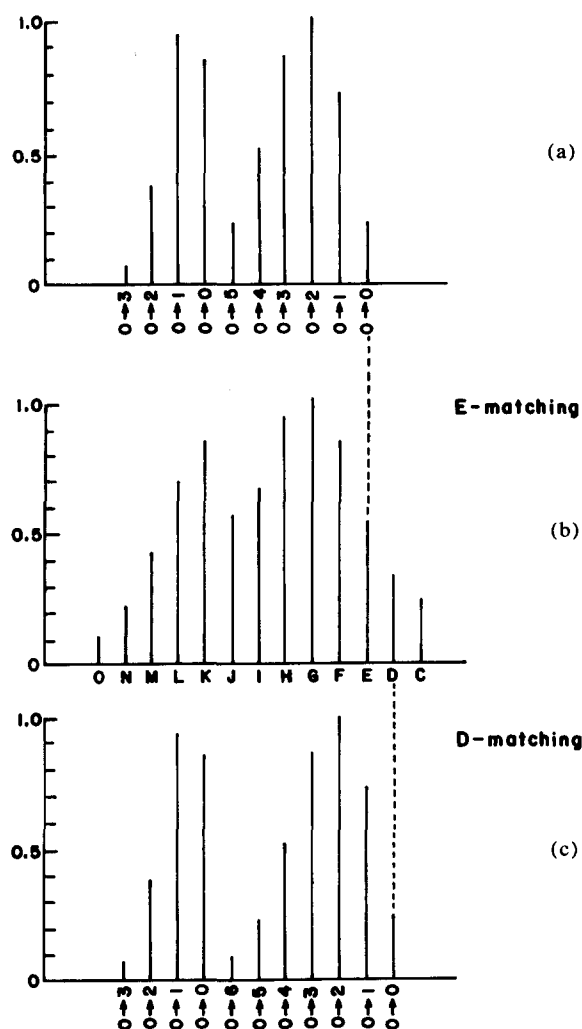


FIG. 7. Comparison of experimental and theoretical FCFs for the PD process HO₂(*X,A*) ← HO₂⁻(*X*). The experimental FCFs of Oakes, Harding, and Ellison are plotted in (b) and the present computed FCFs for the main or "cold" $v'(X,A) \leftarrow v'' = 0(X)$ vibrational progressions are plotted in (a) and (c) so as to depict the E and D matchings (see the text).

ground state would be 2.06–0.87 or 1.19 eV, which would be the adiabatic electron affinity of HO₂(*X*).⁷ The KE corresponding to this value is 1.35 eV (2.54–1.19 eV). Hence, either peak E at 1.295 eV or D at 1.407 eV might be assigned as the origin of *X* on this basis.

The interpretation of Oakes *et al.*⁸ is based on the assumption that peak K at 0.590 eV is the origin of the *A*-state progression, i.e., that K results from the $A \leftarrow X^- 0 \leftarrow 0$ transition. Peaks L, M, and N were assigned accordingly as 1 ← 0, 2 ← 0, and 3 ← 0. The choice of K as the *A*-state origin fixes the assignment of the *X*-state structure as well. This was done by employing again the experimental HO₂(*A-X*) splitting of 0.871 eV, thus obtaining a KE value of 1.461 eV (0.590 + 0.871 eV) for the expected position of the *X*-state origin. Both peaks C (1.503 eV) and D (1.407 eV) are viable candidates on this basis, although neither one of them correspond exactly to 1.461 eV. Oakes *et al.* chose peak D as the $X \leftarrow X^- 0 \leftarrow 0$ transition and assigned peaks E, F, ..., J accordingly as 1 ← 0, 2 ← 0, ..., 6 ← 0.

The assignment of the observed HO₂⁻ PES structure

according to the present FCF calculations is as follows. The assignment of the peaks belonging to the $A \leftarrow X^-$ band system is made by finding the best fit of the computed $v'(A) \leftarrow v'' = 0$ FCFs with the intensity profile of measured peaks K through N assumed to correspond to the *A* state of HO₂. It seems quite consistent that the two largest (and nearly equal) FCFs which correspond to the 0 ← 0 and 1 ← 0 transitions should be assigned to peaks K and L, respectively, which are the strongest of the second observed progression. This fact suggests that peak K is the origin of the $A \leftarrow X^-$ band system. Accordingly, our FCF for the 0(*A*) ← 0 transition was adjusted to the experimental FCF of peak K (0.85), and those of the remaining vibrational features in the progression were adjusted proportionally. The assignment of the *A*-state features consistent with this choice of origin is: K(0 ← 0), L(1 ← 0), M(2 ← 0), and N(3 ← 0).

For the $X \leftarrow X^-$ system the most straightforward means of matching the measured and calculated peak intensities is to equate the largest calculated FCF to that of the most intense measured feature, adjusting the theoretical FCFs of the remaining peaks accordingly. The vibronic transition with the largest calculated FCF is found to be 2 ← 0, and it is thus associated with the FCF of peak G (1.0), the strongest in the measured spectrum. From this choice it follows that peak F would correspond to the 1 ← 0 transition and peak E to the 0 ← 0 species (E matching, Fig. 7). An alternative matching between computed and measured FCFs is possible, however, as a result of the rather large uncertainty ($\pm 30\%$, Ref. 8) embodied in the experimental FCFs. Otherwise, only a slight adjustment of the computed FCFs of two pairs of transitions with calculated ratios of 1.0:0.86 ($X \leftarrow X^-$) and 0.85:0.93 ($A \leftarrow X^-$) is required to match the most intense PES peaks with the largest theoretical FCFs in those two bands so as to obtain perfect agreement with the assignment favored by Oakes *et al.* Such an adjustment of the computed FCFs is consistent with the level of vibrational treatment employed in the present work. The alternative matching, denoted D matching in Fig. 7, is the one preferred by Oakes *et al.* The important point to notice here is that in virtue of the large error bars of the measured FCFs the present computed FCFs for the $X \leftarrow X^-$ band fit reasonably well the recorded spectrum also when peak D is taken as the origin (Fig. 7). In the following section it will be shown that neither assignment of peak E or D as *X*-state origin is without difficulty, however.

VI. DISCUSSION ON THE INTERPRETATION OF THE HO₂⁻ PES

The peaks which qualify as origins of the *X* and *A* band systems on the basis of the experimental^{7,8} and present theoretical results are collected in Table V. There appears to be a

TABLE V. Peaks likely to be the origins of the *X* and *A* states (as suggested by experimental and theoretical data).

	Origin of <i>A</i>	Origin of <i>X</i>
Threshold photodetachment (Ref. 7)	K or L	E or D
Photoelectron spectroscopy (Ref. 8)	K	C or D
Theoretical (this work)	K	E or D

consensus regarding the origin of the *A* state, with all studies pointing to peak K. The photodetachment experiment indicates a KE value of 0.48 eV for this 0←0 transition as compared with the position of peak K in the spectrum at 0.590 eV. As mentioned above, the choice of Oakes *et al.* of peak K as origin is simply based on the appearance of the profile of peak intensities: the break between the *A*←*X*⁻ and *X*←*X*⁻ progressions appears to occur between K and J. The present theoretical assignment is also partly based on the general appearance of the spectrum, but there are additional considerations which lend further support to this interpretation. One important point is that both experimental and theoretical evidence indicate that there are only two peaks of large and roughly similar intensity, namely (K,L) or (0←0,1←0) which can be associated with the *A* system. The peaks neighboring them on both sides, J on the right of K and M on the left of L are considerably smaller. This fact in itself makes it difficult to conceive a matching for the *A*←*X*⁻ features other than the one indicated in Fig. 7.

That peak J is unlikely to be associated with the origin of *A* is also supported by the following observation, namely that the (J,K) interval of 669 cm⁻¹ is too small to correspond to the *A* state, whose characteristic ν₃(O—O) vibrational frequency is 926 or 986 cm⁻¹ (Table III). By contrast, the intervals K—L (992 cm⁻¹), L—M (960 cm⁻¹), and M—N (968 cm⁻¹) are clearly much closer to the ν₃(*A*) value. This fact thus also supports the choice of peak K as being the first of the main (*v*'←*v*"=0) *A*-state progression. Nonetheless, it should be noticed in this connection that peak positions in Ref. 8 were placed at the center of gravity of the spectral features²⁰ (including those of peaks displaying an unusually large width and/or irregular shapes), so the positions of the peaks (for example, J at 0.673 ± 0.019 eV) are somewhat uncertain, thus perhaps affecting the validity of the above argument pertaining to the size of the (J,K) splitting.

The location of the origin of the *X*←*X*⁻ band system is more difficult to determine. The photodetachment data⁷ and the present FCFs support either peak E or D as this origin, whereas the PE data favor D or C. We have seen in Sec. V D that the present computed *X*←*X*⁻ FCFs fit the measured spectral features satisfactorily when either peak E or peak D is taken as the *X*-state origin. No reasonable agreement is found between computed and measured spectra when peak C is taken as the origin of the *X* state (incidentally, such an assignment would yield a K—C splitting of 0.913 eV in good agreement with the corresponding *A*←*X* *T*₀ value of 0.871 eV), however. Therefore according to the present theoretical evidence only peaks E and D qualify as possible *X*-state origins. Either option presents both advantages and drawbacks, however. Taking peak E as origin results in a nice matching between measured and theoretical spectra, i.e., the overall features of the recorded spectrum are fairly well reproduced by the present FCFs [compare Figs. 7(b) and 7(a)], but the K—E energy splitting is only 0.705 eV, as compared with the optical HO₂ *A*←*X* *T*₀ energy of 0.871 eV. Choosing peak D as origin yields a better *A*←*X* *T*₀ value (but still too small as the K—D gap is only 0.817 eV), but at the same time the matching of measured [Fig. 7(b)] and computed [Fig. 7(c)] spectra is somewhat less satisfactory.

The inconsistencies associated with the choices of E or D (and ultimately with the recorded spectrum itself) can also be seen from the fact that different HO₂ EAs can be inferred from the measured spectrum depending upon which criterion is employed to obtain them. The EA inferred from the choice of E as origin is 1.245 eV (2.540 — 1.295 eV), whereas that deduced taking D is 1.133 eV (2.540 — 1.407 eV). These two values of the electron affinity obtained from spectral data disagree with the recommended EA(HO₂) = 1.078 ± 0.017 eV of Oakes *et al.*, which is obtained by simply adding the known *A*←*X* *T*₀ energy of 0.871 eV to the KE of peak K (0.590 eV) and then subtracting the sum of 1.461 eV from the photon energy (2.540 eV). The preferred EA = 1.078 of Oakes *et al.* appears to be quite reliable, however. Indeed, a series of calculations on four closely related neutral-anion pairs yields an estimate of the HO₂ EA of 1.069 ± 0.05 eV,⁶ in excellent agreement with this value. Moreover, it should be emphasized that this theoretical estimate is independent of the FCF calculations and therefore constitutes an additional piece of information supporting a value of 1.078 eV for the electron affinity of HO₂.

In order to gain a deeper insight into the origin of the discrepancies mentioned above it is worthwhile to analyze in more detail some pertinent aspects of the theoretical and experimental studies. The first consideration is whether the overall theoretical treatment is of suitable reliability in the present study, but there is strong evidence that this is the case: (1) The O—OH equilibrium bond lengths and the related ν₃ vibrational frequencies of the three curves involved in the PD process agree quite well with the experimental counterparts (see Tables I and III); (2) the calculated adiabatic HO₂ *A*←*X* splitting of 0.91 eV (which is clearly independent of the above vibrational assignments) is quite close to the experimental value of 0.871 eV; and (3) the overall features of the measured spectrum are fairly well reproduced by our FCFs (Fig. 7).

A point which also bears scrutiny pertains to the accuracy and reliability of the electron KE measurements (and/or electron counting) in the experiments. This point was first raised in connection with the possibility that the energy splitting between peaks could have been underestimated. Evidence of some sort of "shrinking" in the KE scale arises from the fact that the splitting between successive peaks of the *X* state is consistently 50–100 cm⁻¹ smaller than the Δν₃ vibrational spacing of HO₂(*X*), which is known accurately from optical measurements to be 1101 cm⁻¹ (Table III). Accordingly, Oakes *et al.* report a harmonic frequency of only 1020 cm⁻¹ for the band system comprising peaks D through J, which at least partially explains why the HO₂ *A*←*X* splitting (i.e., the K—D energy gap) is significantly underestimated in their spectrum.

It is perhaps also well to note that there are some controversial experimental facts regarding peak D: (1) it (as well as peak C) does not show up in the low signal-to-noise spectrum and is only barely perceptible in the high signal-to-noise recording (see Figs. 4 and 5 of Ref. 8). This behavior stands in contrast with all other *X*-state peaks, E through J, which are much more intense and quite distinct; (2) the D—E vibrational interval of 903 cm⁻¹ is significantly smaller

than the E-F, F-G, G-H, and H-I intervals (Table II), which we believe can be safely ascribed to *X*; (3) according to the mass spectral data (see Fig. 2 of Ref. 8) the mass separation was not completed properly, so there may exist some O₂⁻ (*m/z* = 32) contamination in the HO₂⁻ (*m/z* = 33) beam; the actual effect of this interference is difficult to assess but, according to Oakes *et al.*, it might distort, broaden, and even slightly shift the peaks, especially C and D; (4) peak D is the feature with the largest uncertainty in peak position (± 0.024 eV); (5) the nonnegligible intensity of peak C (most probably associated with a hot band) might indicate that D is a composite peak involving a number of vibronic and rotational transitions. In view of the above observations and given the somewhat elusive and dubious nature of peak D, it therefore can not be excluded that this feature may not belong to the main HO₂ (*X*, *v'* ≥ 0) ← HO₂⁻ (*X*, *v''* = 0) progression, but rather could perhaps better be associated with a hot-band transition.

VII. ON THE ROLE OF HOT TRANSITIONS IN THE HO₂⁻ PES

We have seen that the experimental HO₂⁻ PES is reasonably well reproduced by the (*X*, *A*) ← *X*⁻ FCFs of the main *v'* ≥ 0 ← *v''* = 0 progression. In the following it will be argued that hot transitions may also contribute significantly to the observed intensity pattern of the PE spectrum. There is no explicit information in the study of Oakes *et al.* regarding the vibrational temperature of the HO₂⁻ beam nor on its equilibrium or nonequilibrium condition. However, the spectrum shows feature C to the right of D, the *X* state origin postulated by these authors, which they assign as the *v'* = 0 ← *v''* = 1 transition of the *X* ← *X*⁻ system; this would require that at least *v''* = 1 be significantly populated, in which case one would have to conclude that the beam is at least to some extent vibrationally and rotationally hot. If the beam were statistically in equilibrium the sole level appreciably populated at room temperature would be *v''* = 0, but since HO₂⁻ was produced collisionally it is not surprising that the beam may be vibrationally excited. According to the present computations a number of hot transitions have large FCFs (Table IV), so they could show up in the spectrum with appreciable intensity if a large number of HO₂⁻ (*v''* > 0) molecules were present in the beam.

According to the discussion of the previous section in which it was argued that the 0 ← 0 *X* ← *X*⁻ transition can be associated with peaks E or D, it seems quite reasonable that peak C lying on the right of D could be associated with a hot transition. If D is taken as the *X* ← *X*⁻ origin the D-C interval would correspond to a quantum of *v*₃ in the HO₂⁻ *X*¹*A*' state, whereby the energy gap between D(0 ← 0) and C(0 ← 1) gives directly the HO₂⁻ (*v''* = 1 ← 0) splitting. It might therefore be significant in this respect that the D-C (774 cm⁻¹) interval is definitely smaller than the F-E, G-F, and H-G gaps of the *X* progression, and thus is closer to *v*₃ (O-O) of HO₂⁻ (present computed value 833 cm⁻¹) than to the neutral counterpart (1101 cm⁻¹). This result thus supports the hot nature of C. As we have seen, the E-D interval of 903 cm⁻¹ is also significantly smaller than the *X*-state intervals thus casting some doubts on whether peak D actu-

ally belongs to the main progression. Nonetheless a more definite statement on these questions must await further experiments.

As we have mentioned before, the significant strength of C indicates that a good portion of the HO₂⁻ molecules are in the *v'* = 1 vibrational state. One can thereby envision the *X* ← *X*⁻ 0 ← 0 transition enlarged by the 1 ← 1, 2 ← 2, ... sequence. The possibility of 1 ← 1 contributing meaningfully to the intensity of 0 ← 0 is supported by the large size of its computed FCF, 0.72; higher members of the sequence appear to be of less importance, their FCFs being small, 0.12 (2 ← 2) and 0.10 (3 ← 3). The energies of 0 ← 0 and 1 ← 1 are somewhat different as a result of the fact that the characteristic vibrational frequencies are distinct in initial and final electronic states. In the present case the 1 ← 1 excitation energy is 268 cm⁻¹ (1101 - 833 cm⁻¹) larger than that of 0 ← 0. Hence an electron detached in the former process should carry less KE away than one associated with the latter, that is to say, 1 ← 1 should occur somewhat to the left of 0 ← 0 in the PE spectrum. It should be noted that the 268 cm⁻¹ energy gap is well within the size of the width at half-height of peak D or E, which we estimate to be not less than 0.1 eV or 800 cm⁻¹ (see Fig. 5 of Ref. 8). It is therefore reasonable to expect that the intensities of the 1 ← 1 and 0 ← 0 transitions augment each other in the spectrum.

Besides peak C other spectral features, such as anomalously large widths, irregular shapes or a multispikes structure of some of the peaks strongly indicate the occurrence of hot transitions. For example, the large widths of E, I, and J, together with their very peculiar profile, suggest they could be composite peaks. Part of their widths (as well as that of all other peaks) can clearly be traced back to the rotational envelope which normally accompanies vibronic transitions; however, much of the line broadening observed in the PES peaks is very probably due to the superposition of various transitions. According to Table IV the most likely species to blend with the *X* ← *X*⁻ 4 ← 0 transition are 5 ← 1 and 6 ← 2, with FCFs of 0.71 and 0.44, respectively. The 6 ← 1, 7 ← 2, and 8 ← 3 species, with FCFs of 0.54, 0.65, and 0.52, could contribute to the intensity of the 5 ← 0 transition. It is also possible that hot transitions to the *A* state contribute intensity to J and I, the most likely candidates being 0(*A*) ← 1 and 0(*A*) ← 2 respectively, with FCFs of 0.75 and 0.40. Finally a comment can be made relative to peak O, which is also not sharp in the spectrum. One would be inclined to associate this feature with the 4 ← 0 member of the *A* ← *X*⁻ system, but its computed FCF is 0.00. Therefore if it does actually arise from HO₂⁻, it is probably also better associated with a hot transition.

A point on which we had hoped to shed light on the basis of the calculated FCFs of hot transitions concerns the difference between experiment and theory regarding the relative intensity of peaks K and L, namely K is stronger in the high signal-to-noise spectrum (notice however that in the low resolution spectrum K and L have similar intensity), whereas the calculations predict the opposite (see Figs. 4 and 5 of Ref. 8). Based on purely qualitative arguments since the *X*⁻ and *A* curves are shifted with respect to each other it seems quite reasonable that the FCF of the 1 ← 0 transition should

be stronger than that of 0←0. The observed trend for the largest calculated FCFs of $X(2←0)$ and $A(1←0)$ is in agreement with what one would expect from the fact that the difference in O–O equilibrium bond length between anion (1.499 Å) and neutral (1.330 Å for X and 1.393 Å for A) is greater for $X←X^-$ than for $A←X^-$. However, no hot transitions appear to be in a position to enhance the $A←X^- 0←0$ transition (peak K). The 1←1, 2←2, and 3←3 transitions of the A system and the cold 6←0 $X←X^-$ transition, which could eventually add their intensity to the 0←0 feature, all have very small FCFs, namely 0.00, 0.13, 0.28, and 0.00. Moreover, a number of hot transitions appear to be capable of enhancing the $A←X^- 1←0$ transition (peak L) instead, i.e., the $A←X^- 2←1$ transition with a FCF of 0.66. Regarding this point it can finally be noted that there is perfect matching between the experimental and theoretical $A←X^-$ band intensity distribution when one takes into consideration the large uncertainty of the measured FCFs.

VIII. CONCLUSIONS

The present *ab initio* CI computations of the intensity distributions in the HO₂⁻ ionization spectrum succeed in giving a satisfactory representation of the corresponding measured data.^{7,8} There are two independent results of our *ab initio* calculations which are supportive of the assignment of the recorded PES structure preferred by Oakes, Harding, and Ellison⁸ and of their HO₂(X) electron affinity value of $1.078 ± 0.017$ eV: (1) The present computed (cold) FCFs for the active mode O–OH reproduce fairly well the overall features of the measured PE spectrum and agree with the assignment of Oakes *et al.* of peaks K and D as vibrational origins of the $A←X^-$ and $X←X^-$ overlapping band systems; (2) it is found that upon making an empirical adjustment to the computed HO₂ electron affinity, as suggested by analogous comparisons between calculated and measured EAs of O, OH, and O₂, a value of $1.069 ± 0.05$ eV is indicated for the HO₂ adiabatic first EA.

While this level of consistency is quite satisfying, it still cannot truly be claimed that the matter is settled, however. On the experimental side, there are inconsistencies which are somewhat too great to justify unqualified confidence in the assignment of the HO₂⁻ PES as well as in the accuracy of the HO₂ EA value given by Oakes *et al.* For example, the K–D energy splitting in their measured spectrum is only $0.817 ± 0.037$ eV, whereas the HO₂ $A←X T_0$ energy from optical measurements is $0.871 ± 0.000 001$ eV; also the observed $\Delta\nu_3$ vibrational splittings of the $X←X^-$ band are underestimated by as much as 80 cm^{-1} . According to the present calculations, an interpretation in which peak E is identified as the $X←X^-$ band origin seems a viable alternative to that of Oakes *et al.* This matching gives better agreement between computed and measured FCFs, but requires associating the measured K–E energy difference of

$0.705 ± 0.031$ eV with the $A←X T_0$ value of HO₂. In view of the above arguments it is clear that there is still some uncertainty in the value of the electron affinity. Further experiments, i.e., a PE spectrum of greater resolution, seem desirable to check the assignment of the PES structure and the accuracy of the HO₂ EA.

ACKNOWLEDGMENTS

The authors are indebted to the Deutsche Forschungsgemeinschaft for the financial support extended to this work within the framework of the Sonderforschungsbereich 42. One of us (G.J.V.) also wishes to thank the SFB 42 for a visiting professor fellowship at the University of Wuppertal, Dr. G. Hirsch for fruitful discussions during the course of this work, as well as Professor B. G. Ellison and Dr. Veronica Bierbaum for personal communications. The computation facilities of the Universities of Bonn and Wuppertal are gratefully acknowledged. Diverse facilities required for the completion of this work were provided by the Instituto de Fisica (UNAM). This work was also supported by CONACYT (Reference p228ccox880438).

¹M. Kaufman and J. Sherwell, *Prog. React. Kinet.* **12**, 1 (1983).

²C. J. Howard, *J. Am. Chem. Soc.* **102**, 6937 (1980).

³S. W. Benson and P. S. Nangia, *Acc. Chem. Res.* **12**, 223 (1979).

⁴G. J. Vazquez, S. D. Peyerimhoff, and R. J. Buenker, *Chem. Phys.* **99**, 239 (1985).

⁵G. J. Vazquez, R. J. Buenker, and S. D. Peyerimhoff, *Mol. Phys.* **59**, 291 (1986).

⁶G. J. Vazquez, R. J. Buenker, and S. D. Peyerimhoff, *Chem. Phys.* **129**, 405 (1989).

⁷V. M. Bierbaum, R. J. Schmitt, C. H. De Puy, P. A. Mead, P. A. Schulz, and W. C. Lineberger, *J. Am. Chem. Soc.* **103**, 6262 (1981).

⁸J. M. Oakes, L. B. Harding, and G. B. Ellison, *J. Chem. Phys.* **83**, 5400 (1985).

⁹C. H. De Puy, V. M. Bierbaum, R. J. Schmitt, and R. S. Shapiro, *J. Am. Soc.* **100**, 2920 (1978).

¹⁰H. Bash and R. Osman, *Chem. Phys. Lett.* **93**, 51 (1982).

¹¹M. S. Morgan, P. F. Van Trieste, S. M. Garlick, M. J. Mahon, and A. M. Smith, *Anal. Chim. Acta* (submitted).

¹²D. Cohen, H. Basch, and R. Osman, *J. Chem. Phys.* **80**, 5684 (1984).

¹³R. J. Buenker, S. D. Peyerimhoff, and W. Butscher, *Mol. Phys.* **35**, 771 (1978).

¹⁴R. J. Buenker and S. D. Peyerimhoff, *Theor. Chim. Acta* **35**, 33 (1978); **39**, 217 (1975).

¹⁵R. J. Buenker, *Studies in Physical and Theoretical Chemistry*, Current Aspects of Quantum Chemistry, Vol. 21, edited by R. Carbo (Elsevier, Amsterdam, 1982), pp. 17–34; Proceedings of the workshop on Quantum Chemistry and Molecular Physics, Wollongong, Australia, February 1980.

¹⁶R. J. Buenker and R. A. Phillips, *J. Mol. Struct. (Theochem)* **123**, 291 (1985).

¹⁷R. McWeeny, *Coulson's Valence*, 3rd ed. (Oxford University, Oxford, 1979), Chap. 4.

¹⁸G. J. Vazquez, *Notas Fis. (UNAM)* **10**, 201 (1987).

¹⁹R. P. Tuckett, P. A. Freedman, and W. T. Jones, *Mol. Phys.* **37**, 379, 403 (1979).

²⁰G. B. Ellison (personal communication).